Influence of ignored and well-known zone distortions on the separation performance of proteins in capillary free zone electrophoresis with special reference to analysis in polyacrylamide-coated fused silica capillaries in various buffers[☆]
I. Theoretical studies

Stellan Hjertén[a,*], Sheila Mohabbati[b], Douglas Westerlund[b]

[a] *Department of Biochemistry, Uppsala University, Biomedical Center, P.O. Box 576, SE-75123, Uppsala, Sweden*
[b] *Analytical Pharmaceutical Chemistry, Uppsala University, Biomedical Center, P.O. Box 574, SE-75123, Uppsala, Sweden*

Abstract

Distortion of the starting zone upon its electrophoretic migration toward the detection window gives rise to both symmetrical zones caused by diffusion, sedimentation in the horizontal section of the capillary and the curvature of the capillary, and asymmetrical zones having their origin in Joule heating, sedimentation in the vertical section of the capillary, pH and conductivity differences between the sample zone and the surrounding buffer, solute adsorption onto the capillary wall, and association–dissociation of complexes between the analyte and a buffer constituent or between analytes. Interestingly and importantly a theoretical study shows that moderate pH and conductivity differences as well as adsorption and all of the above interactions when they are characterized by a fast on/off kinetics do not increase the zone broadening (or only slightly), because the sharpening of one boundary of the zone is about the same as the broadening of the other boundary. In addition the peak symmetry caused by a conductivity difference is in most experiments counteracted by a pH difference. The experimentally determined plate numbers in the absence of electroosmosis exceeded one million per meter in some experiments (Part II). These plate numbers are among the highest reported [Z. Zhao, A. Malik, M.L. Lee, Anal. Chem. 65 (1993) 2747; M. Gilges, K. Kleemiss, G. Schomburg, Anal. Chem. 66 (1994) 2038; H. Wan, M. Öhman, L.G. Blomberg, J. Chromatogr. A 924 (2001) 59] (plate numbers determined in the presence of electroosmosis may be higher, although the width of the zone in the capillary may be larger) [p. 680 in S. Hjertén, Electrophoresis 11 (1990) 665]. Capillary free zone electrophoresis is perhaps the only separation method, which, under optimum conditions, gives a plate number not far from the theoretical limit. A prerequisite for this high performance is that the polyacrylamide-coated capillary is washed with 2 M HCl between the runs and stored in water over night (Part II). The difference between the experimentally determined total variance and the sum of the calculated variances originating from the width of the starting zone, longitudinal diffusion, Joule heating, sedimentation in the vertical section of the capillary, curvature of the capillary (i.e., the sum of all other variances) was in our most successful experiments about 28% of the variance of diffusion. The zone broadening, 2σ, caused by diffusion was estimated at 0.77 mm. The total zone width (2σ) calculated from the experimentally determined plate number was as small as 1 mm when the migration distance was 40 cm. Accordingly, the only efficient way to reduce drastically the total zone width is to decrease the analysis time and, thereby, the diffusional broadening. An important finding was that the variance originating from the loops of the capillary is not always negligible in high-performance runs. Therefore, one should employ straight capillaries and avoid CE apparatus with cartridges that require a strong curvature of the capillary, common in most commercial instruments. Mathematical formulas have been

---

derived for the sedimentation of the solute zone, the enrichment factor, and the migration time in experiments where the solute is dissolved in a dilute running buffer. This zone sharpening method gave very narrow starting zones (0.04–0.4 mm). However, upon high dilution of the buffer the enrichment becomes so strong that part of the sample zone probably sediments out of the capillary; the almost inevitable change in pH may decrease the mobility of the proteins and, thus, cause the enrichment factor to become still lower than expected. Diffusion of the protein in the very narrow starting zone (located close to the tip of the capillary) and sometimes the thermal expansion of the buffer in the capillary contributes to additional loss of protein in the enrichment step. In some buffers, the interaction between the protein and the buffer constituents is so slow that the peaks become broad. Therefore, different types of buffers should be tested when high resolution is required. The relation σ^2 (the variance of the interaction between a protein and the buffer constituents) = constant $\times u$ (the mobility) seems to be valid for all proteins in the applied sample, at least when they have similar molecular masses. To facilitate the understanding of the progress of a free zone electrophoresis experiment, we have discussed in simple terms how the concentrations of the background electrolytes become rearranged during a run and why the difference between the mobilities of the proteins and the mobilities of the background electrolyte determines whether a peak exhibits fronting or tailing. A theoretical analysis of zone broadening in capillary zone electrophoresis, chromatography, and electrochromatography indicates that electrochromatography in homogeneous gels might be the only chromatographic technique which can compete in performance with free electrophoresis. Using an equation, valid not only for electrophoresis, but also for chromatography and centrifugation, the mobility of a concentration boundary has been calculated for the first time and was, as expected, low. Equations based on the Kohlrausch regulating function do not permit such calculations. Another regulating function (the H function) and some of its characteristics are briefly discussed. The theoretical discussions in this paper and the experimental studies in Part II show that high-performance electrophoresis deserves its prefix when the runs are designed to give minimum zone broadening. Some guidelines are given to facilitate this optimization. The plate numbers are so high that the resolution cannot be increased by more than 30% even if they approach the theoretically maximum values.

1. Introduction

In the preliminary phase of a study on the behavior of proteins in capillary free zone electrophoresis at low pH and with on-line concentration of the proteins based on their solubilization in the diluted running buffer, several interesting observations were made. For instance, the plate numbers were in some experiments far above one million per meter, despite the fact that the peaks exhibited tailing. Furthermore, the peak heights and the peak areas were about the same or lower when the proteins were injected in the running buffer diluted more than 100- or 200-fold (Part II [1]). In addition, in the very first experiments the electrophoresis patterns were not reproducible in some of the buffers. Therefore, we decided to perform this theoretical study aimed at finding out which separation parameters that were of particular importance to explain these unexpected observations with our hope that the investigation would contribute to a better knowledge of optimum separation conditions and, therefore, to a general improvement of the capillary free zone electrophoresis technique.

It soon appeared that the current theory of known zone broadenings could not explain all of the above observations. Therefore, we decided to describe quantitatively the total width, generally in the form of the variance, of an electrophoretic zone in terms of known functions (such as those for the width of the starting zone, diffusion, Joule heat, adsorption, conductivity differences, the curvature of the capillary), as well as functions not, or only slightly, treated theoretically earlier (pH differences, sedimentation of a sample zone, slow association–dissociation of a complex between the analyte and a buffer constituent, weak reversible adsorption onto the capillary wall).

To get a quantitative picture of the enrichment degree of the proteins in the on-line concentration method used herein, the research program also included the derivation of a relevant equation.

Access to an equation for the migration time was also required, since it could not be calculated in the conventional way because the field strength in the low-conductivity plug originating from the application of the sample in dilute buffer is much higher than that in the rest of the capillary. For the same reason, a non-conventional method was required for the estimation of the width of the starting zone. The derivation of some of the equations presented will not be given to avoid making the paper excessively long.

The separation mechanisms of electrophoresis, chromatography, and electrochromatography are analogous because they are based on the same parameter, namely the migration velocity of the analyte. Analogous separation profiles can, accordingly, be expected.

2. Theory with some experimental links

2.1. The width of the starting zone (ΔX_0) and its variance ($\Delta X_0^2/12$)

ΔX_0 $(= \sqrt{12}\sigma)$ cannot be calculated in the conventional way from the migration velocity and the time of application of the sample when the zone sharpening method is used to create a narrow starting zone, i.e., when the sample has an electrical conductivity lower than that of the background electrolyte, because: (1) the field strength in the sample zone is much higher than that in the rest of the capillary, and (2) the boundary between the non-diluted and diluted buffer, being a

(A)

(B)
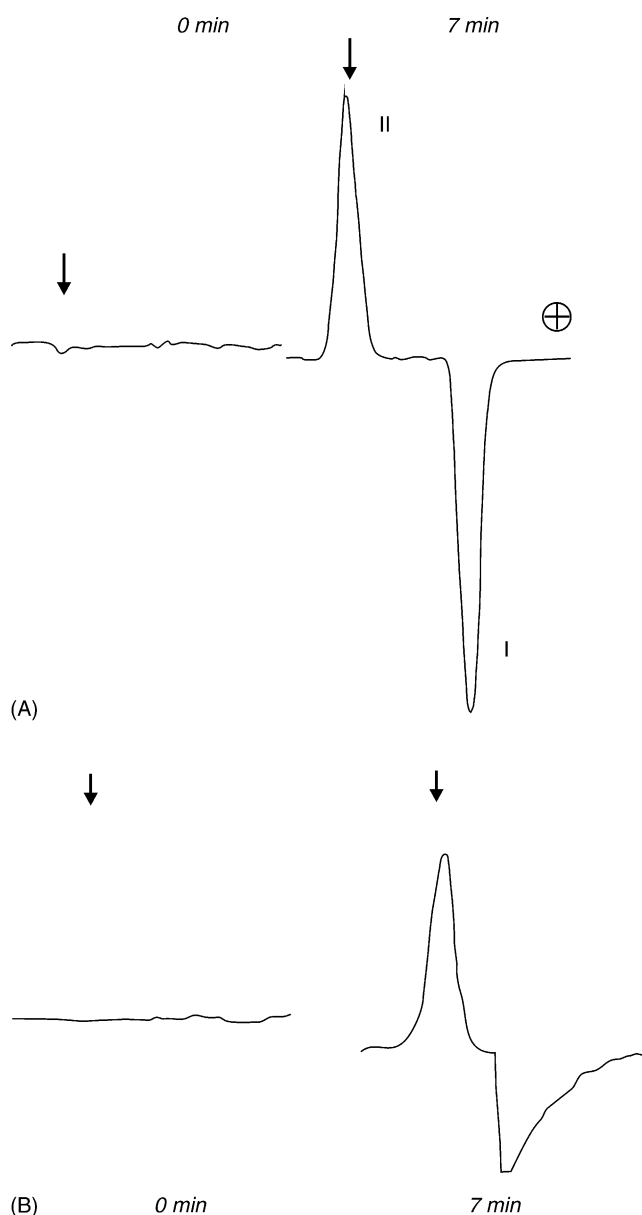
Fig. 1. Local alterations in the buffer concentrations upon electrophoresis. Analysis method: free zone electrophoresis [4,13]; buffer (UV-absorbing): sodium veronal, pH 8.6; sample (non UV-absorbing): sodium cacodylate (experiment A) and sodium sulfate (experiment B); detection: UV scanning of the capillary. The arrow indicates the position of the application of the sample. The electropherograms show that there is a change in the buffer concentration (in these experiments an increase) where the sample was applied and also in the migrating sample zone (in this case a decrease) in accordance with the discussion in Sections 2.5.1, 2.5.2 and 2.5.3. The electropherograms are reproduced with permission from the author and the publisher.

concentration boundary, is virtually stationary (see Fig. 1 and Section 3.7). In this particular case, the following approach can be employed when diffusion is the only parameter causing zone broadening:

$$H = \frac{\Delta X_0^2}{12 L_d} + \frac{2D}{uE} \tag{1}$$

where D and u are the diffusion constant and the mobility of the protein, respectively, and L_d is the length of the capillary to the detection window. ΔX_0 can be estimated from a plot of the total plate height, H, against $1/E$ (Fig. 9a in Ref. [2]), where E is the field strength in the buffer zone, which, for the above reasons, must be calculated from the relation $E = (I/\kappa q)$ (I is the current, κ the electrical conductivity, and q the cross-sectional area of the capillary), and not from $E = (V/L_t)$. This plot can be used only under certain experimental conditions (p. 681 in Ref. [2]), which are fulfilled if the plot gives a straight line (Fig. 9a in Ref. [2]). If not, the experiment should be repeated at a lower field strength to suppress zone distortions, which are a function of the field strength, in an attempt to approach a linear plot [observe that the broadening caused by sedimentation then increases since the migration time increases (Eq. (13)]. Interestingly, this plot also permits a determination of the universal constant D/u (Eq. (1) herein and p. 681 in Ref. [2]) and, consequently, the diffusion constant, since the mobility can easily be calculated. Alternatively, if D of the analyte is known, the slope can be calculated. In this case, it is sufficient to determine the plate height at one (low) field strength. Using the latter approach ΔX_0 was estimated at 0.04–0.4 mm in the experiments described in Part II [1]. The method of zone sharpening thus gives very narrow starting zones (see Section 3.7 for further discussion).

2.2. Longitudinal diffusional broadening

This broadening is determined by the Einstein equation:

$$\sigma_{diff}^2 = 2Dt = 2D\frac{L_d}{uE} \tag{2}$$

where L_d is the length of the capillary to the detection window and t the migration time. When the diffusion constant is not known, the parameter (D/u) can be estimated as described in the previous section.

2.3. Thermal zone broadening

The variance, σ^2, of the thermal zone broadening is determined by the expression (Eqs. (53b) and (6b) in Ref. [2]):

$$\sigma_J^2 = \frac{1}{12}(\Delta x_j)^2 \tag{3}$$

where Δx_j is the maximum thermal zone broadening. Δx_j can be replaced by Eq. (6b) in Ref. [2] (see also Eq. (73) in Refs. [3,4]):

$$\sigma_J^2 = \frac{1}{12}\left[\frac{B\kappa L_d}{\lambda}\frac{RE}{2T_0}\right]^2 \tag{4}$$

Using an intuitive simple approach, one can show that this relationship, upon superimposition of radial diffusion, is

transformed to [5]:

$$\sigma^2_{J,\,\text{rad diff}} = \frac{1}{12}\left[\frac{B\kappa}{\lambda}\left(\frac{RE}{2T_0}\right)^2\right]^2 \frac{L_d^2}{t}\frac{R^2}{8D} \tag{5}$$

where $B = 2400$ K, κ the electrical conductivity, λ the thermal conductivity of the buffer, R the radius of the capillary, and T_0 the temperature of the coolant. Following some obvious transformations Eq. (5) is exactly the same as that derived by Virtanen [6], employing the Taylor approach [7]; see also Ref. [8].

An increase of the temperature in the capillary increases the longitudinal diffusional band broadening (Eq. (2)) due to the increase of the diffusion constant, D, which is further discussed in Part II [1]. The term $(R^2/8D)$ is the time for a molecule to diffuse radially the distance $R/2$.

2.4. Zone broadening caused by adsorption onto the capillary wall

The variance is determined by Eq. (6) [9] and similar expressions ([10–12]; see also these Refs. and Ref. [8] for other types of zone broadening):

$$\sigma^2_{\text{ads}} = CuE \tag{6}$$

where C is a constant for a given analyte. Accordingly, characteristic of adsorption is that the variance (the width) of a zone, corresponding to a certain protein, increases upon an increase in field strength and also the asymmetry (tailing) of the corresponding peak. Consequently, it is likely that the adsorption is weak or negligible if the total variance decreases when the field strength increases. Observe that the variance of diffusional broadening also decreases upon an increase in field strength. The above criterion for negligible adsorption is, therefore stronger if the total variance is exchanged for the rest variance, as defined in Table 1 (see Section 3.3).

The conclusion drawn in the next section that the resolution between two adjacent peaks need not necessarily decrease for conductivity- or pH-based distortions is true also for adsorption of proteins when the on/off kinetics is fast (see Section 3.2).

Observe that the above statements are, at least qualitatively, also correct for other interactions a protein may be involved in, for instance protein/buffer interactions.

2.5. Zone distortion caused by differences in electrical conductivity between the sample zone and the surrounding buffer ($\Delta\kappa$)

2.5.1. A quantitative treatment

The following relation holds for the solute zone [13,14]:

$$\Delta\kappa = \frac{c_p}{u_p}(u_A - u_p)(u_R - u_p) \tag{7}$$

where $\Delta\kappa$ is the difference in conductivity between the sample zone and the buffer (background electrolyte, BGE), c_p the concentration of the solute zone (coulombs per ml), u_A, u_p, u_R the mobilities of the co-ion (i.e., the buffer ion having the same sign ($+$ or $-$) as the protein), the protein and the counter ion, respectively. The mobility and the ion concentration are signed quantities, positive for cations and negative for anions. It should be noted that the asymmetry of a peak often increases with increasing $\Delta\kappa$ (see Fig. 3 in Ref. [2]), but not always because of the compensating effect of pH differences and possible interactions between the analyte and the buffer constituents (see Sections 2.7 and 2.8). To minimize $\Delta\kappa$, i.e., the asymmetry of a peak (see the next section), the concentration of the protein (c_p) should be as low as possible for reliable detection and adequate precision. The co-ion should be selected so that its mobility is close to that of the protein and the mobility of the counter ion should be low. Interestingly, zone broadening caused by differences in conductivity

Table 1
Experimentally determined total variance, calculated variance, rest variance and zone width/zone broadening

	0.12 M ammonium acetate (pH 4.0) ($N = 1\,600\,000$ m^{-1})		0.15 M ammonium hydroxyacetate (pH 4.0) ($N = 1\,660\,000$ m^{-1})	
	σ^2 (cm^2)	Zone width/zone broadening[a] (mm)	σ^2 (cm^2)	Zone width/zone broadening[a] (mm)
$\sigma^2_{\text{tot,exp}}$	2.50×10^{-3}	*1.00*	2.41×10^{-3}	*0.98*
Calculated values				
$\quad\sigma^2_{\Delta x_0}$	3.20×10^{-6}	*0.062*	No data	*No data*
$\quad\sigma^2_{\text{diff}}$	1.50×10^{-3}	*0.77*	1.43×10^{-3}	*0.76*
$\quad\sigma^2_{J,\text{rad diff}}$	3.04×10^{-6}	*0.035*	7.21×10^{-6}	*0.054*
$\quad\sigma^2_{\text{sed}D}$ [b]	3.39×10^{-8}	*0.0037*	3.39×10^{-8}	*0.0037*
$\sigma^2_{\text{curv},540°}$	2.16×10^{-4}	*0.32*	2.16×10^{-4}	*0.32*
$\sigma^2_{\text{rest}} = \sigma^2_{\text{tot,exp}} - \sigma^2_{\text{calc}}$	0.78×10^{-3}	*0.41*	$\approx 0.75 \times 10^{-3}$	*0.53*

Sample: α-chymotrypsinogen (0.1%), dissolved in 10-fold diluted buffer. Voltage: 17.5 kV, polyacrylamide coated capillary; length to the detector: 40 cm (for further information see Part II [1]).

[a] 2σ, except for ΔX_0 ($\sqrt{12}\sigma$).

[b] The variance for sedimentation in the vertical section of the capillary ($t = 5$ min).

is independent of the field strength (see Eq. (7)). Observe that the mobilities of all ionic species in Eq. (7) increase with dilution of the buffer (Eq. (19)) and the mobilities of proteins increase more than those of the buffer ions by virtue of the larger radii (Fig. 12 in Ref. [2]). For restrictions in the application of Eq. (7), see Section 3.8 and Ref. [13]).

The zone broadening, ΔX_κ, is determined by Eq. (8) (Eq. (19) in Ref. [2]) when the conductivity difference is so large that one boundary of the sample zone remains hyper-sharp during the run whereas the other boundary becomes successively broader (pp. 671–673 in Ref. [2]), which is more seldom the case. A hyper-sharp boundary in an electropherogram or chromatogram is easy to recognize, since it corresponds to a peak where the advancing or rear profile is a straight line perpendicular to the baseline, i.e., the diffusional broadening at one boundary is entirely counteracted by the zone sharpening caused by the conductivity difference. Observe that a hyper-sharp boundary originating from a conductivity or pH difference may be blurred and thus "hidden" by distortions from Joule heat and sedimentation.

$$\Delta X_\kappa = L_d \frac{\Delta \kappa}{\kappa} \tag{8}$$

More often, the conductivity difference is so small that *both* boundaries become blurred. In this case, the retarding effect of the conductivity difference on the broadening at one boundary is compensated almost entirely by the accelerating effect at the other boundary, i.e., the zone broadening caused by a conductivity difference is close to zero (p. 670 in Ref. [2]). The negative effect is the generation of asymmetrical peaks. Fortunately, this will not cause any (or only a small) loss in the resolution of two adjacent peaks (p. 670–671 in Ref. [2]), and will not affect the zone width significantly, or expressed differently, the broadening of one boundary of a zone is compensated by a sharpening of the other boundary (see Fig. 8b and Section 3.6). However, to avoid the risk that a small peak may be hidden in the tailing or fronting part of a larger peak it is important, for example in purity studies of drugs and proteins, to regulate the shape of the latter peak [15] using Eq. (7) to choose buffer constituents with appropriate mobilities. The shape of the small peak will then become similar to that of the large peak, since the mobilities of the two adjacent analytes are similar or, likely, more symmetrical since the concentration is much lower (Eq. (7)).

2.5.2. Physical model picturing qualitatively the local changes in the buffer concentration upon electrophoresis—a qualitative discussion of the implications of Eq. (7)

This equation, like all mathematical formulae, gives only the relation between the embodied parameters and does not explain why the concentrations of the buffer constituents in the stationary zone where the sample was applied and in the migrating sample zone differ from those in the original BGE. However, the following qualitative discussion gives a picture of what actually happens, thereby making it possible

to predict rapidly how the appearance of an electropherogram will change upon a change of relevant parameters (concentration of the sample and the mobilities of the sample and background electrolytes), for instance, to decrease the asymmetry of a peak. This approach is particularly important when Eq. (7) or similar equations cannot be employed because information about the protein concentrations and mobilities is not available, which often is the case.

To simplify the discussion, we assume that the sample has been dissolved in the electrophoresis buffer and is injected by pressure. Upon application of the voltage, the sample zone leaves the starting zone. The treatment below refers to an electrophoresis experiment in an ammonium acetate buffer, a background electrolyte used in some of the experiments presented in Part II [1]. The sample consists of a positively charged analyte and the co-ion, the ammonium ion, has a mobility higher than that of the analyte. It is conceivable that the presence of the positively charged analyte ion in the migrating zone is compensated by a decrease in the concentration of the positive ammonium ions in order to fulfill the requirement that the current (proportional to the number of charges passing a cross section of the capillary per second) must be the same in the cross-sections through the analyte zone and a segment of the surrounding analyte-free buffer. The electroneutrality condition requires that also the concentration of the counter ion, the acetate ion, decreases. This decrease in the concentration of ammonium acetate in the migrating protein zone must result in an increase in the concentration of this salt somewhere else in the capillary, since the total amount of ammonium acetate in the capillary has to be the same before and after the voltage is applied. One can expect the enrichment of ammonium acetate to take place in the stationary zone as the analyte is leaving it.

2.5.3. A visual experimental description of Eq. (7) and a verification of the above qualitative discussion

The examples are taken from Refs. [3,4,13] where a veronal buffer (UV-absorbing) was used in order to permit indirect detection. In both experiments in Fig. 1, a peak was formed where the sample was applied (at the arrow). The electropherograms show that this so-called salt peak is virtually stationary (which is confirmed theoretically in Section 3.7) and corresponds in this case to a buffer concentration higher than that of the surrounding bulk buffer, since the peak is "positive". In the migrating cacodylate zone (experiment A) the buffer concentration is lower than that in the surrounding bulk buffer, since the peak is "negative". Observe that the cacodylate peak is symmetrical, whereas the sulfate peak (experiment B) is asymmetrical, indicating that the mobility of the cacodylate ion differs less from that of the veronal ion than from that of the sulfate ion according to the discussions of Eq. (7) in Section 2.5.1. The fact that the asymmetry is reflected in pronounced fronting indicates that the absolute mobility of the sulfate ion is much higher than that of the veronal ion. A further conclusion can be drawn from this figure; namely, that the finding that the absolute mobility of

the cacodylate ion differs from that of the veronal ion can be made more precise by stating: the difference must be small, since the asymmetry of the peak is small. All of the above conclusions are based on an electrophoresis experiment with small ions, but are valid also for proteins.

2.5.4. Calculation of the valency, z, of a protein

To calculate $\Delta\kappa$ in Eq. (7) and similar equations the valency, z, of the protein must be known, since the protein concentration, c_p, is expressed in coulombs ml^{-1}:

$$c_p = \frac{zM_P F}{1000}$$

where M_P is the concentration of the protein in mol/l and F is the Faraday constant (=96 600 coulombs).

The equation (Eq. (86b) in Ref. [2], valid at 295 K)

$$\frac{D}{u} = \frac{0.025}{z} \tag{9}$$

permits a rough estimation of the valency from an experimental determination of D/u, for instance by plotting plate height against $1/E$, as outlined in Section 2.1 (Part II [1]).

Alternatively, when the diffusion coefficient is known a simple determination of the mobility gives directly information about the valency to be used in Eq. (7) and similar equations.

2.6. Zone broadening caused by differences in pH (ΔX_{pH}) between the sample zone and the surrounding buffer

The following approximate equation is analogous to that which is valid for differences in conductivity (Eq. (8) herein and Eq. (20) in Ref. [2]):

$$\Delta X_{pH} = L_d \frac{\Delta v}{v} \tag{10}$$

where v is the velocity of the protein and Δv is the difference in velocity of the protein in the α- and β-phases due to pH differences. This equation is valid only when the pH difference between the zones is so large that one boundary of the zone remains sharp during the run, i.e., is hyper-sharp, whereas the other boundary becomes continuously broader as the run proceeds. At a pH difference so small that both boundaries become blurred, the retarding effect of the pH difference on the diffusional broadening at one boundary is approximately compensated by the accelerating effect at the other boundary, i.e., the broadening caused by pH differences is close to zero (the reasons are analogous to those used to show that zone distortions caused by conductivity differences are negligible (see Section 2.5.1)). The zone distortion caused by a difference in conductivity may counteract or reinforce that created by a pH difference [16,17]. However, for proteins they act in most cases in opposite directions (see Section 2.7). The pH distortion is independent of the field strength.

2.7. Peak asymmetry caused by a conductivity difference is in most experiments counteracted by a pH difference

2.7.1. Peak asymmetry caused by a conductivity difference ($\Delta\kappa$)

Assume that we do an electrophoresis experiment in a buffer A^+B^- and that the sample consists of four positively charged proteins (p_1, p_2, p_3, and p_4) with the mobilities $u_{p_1} > u_{p_2} > u_{p_3} > u_{p_4}$. The electrophoretic analysis of cytochrome C, lysozyme, ribonuclease A and α-chymotrypsinogen A in an ammonium acetate buffer (pH 4, ionic strength 0.12 M), described in Part II [1], fulfills these requirements.

To facilitate somewhat the theoretical treatment, we write Eq. (7) in the form $\Delta\kappa = c_p(u_A - u_p)((u_R/u_p) - 1)$

Upon a decrease of the protein mobility, $u_A - u_p$ becomes more positive and $(u_R/u_p) - 1$ more negative (see sign rules in Section 2.5.1), which means that $\Delta\kappa$ will become more negative. Therefore, the peak asymmetry (tailing) becomes more pronounced the lower the mobility of the four proteins, i.e., the longer their migration times.

2.7.2. Peak asymmetry caused by a pH difference (ΔpH)

In general, the higher the isoelectric point (pI) of a positively charged protein, the higher its mobility at a pH < pI. We assume, therefore, that the first peak in an electropherogram represents protein p_1, the second peak protein p_2, etc. An ampholyte (for instance a protein) dissolved in deaerated water gives a pH of the water solution, which is close to the pI of the ampholyte. Therefore, the pH in all these protein zones is higher than the pH of the surrounding buffer, i.e., this pH difference causes fronting which is larger the higher the mobility of the protein. Peak p_1 (p_4) has, accordingly, the largest (smallest) fronting, caused by differences in pI, but the lowest (highest) tailing caused by conductivity differences. The conclusion is that the peak distortion caused by conductivity differences often is compensated (more or less) by pH differences.

Using the same approach for negatively charged proteins, assuming that $|u_B| > |u_{p_1}| > |u_{p_2}| > |u_{p_3}| > |u_{p_4}|$ and the buffer pH > pI_{p_4} > pI_{p_3} > pI_{p2} > pI_{p_1} of the proteins, this mobility difference will make $\Delta\kappa$ more negative the lower the $|u_p|$, i.e., cause tailing which is larger for slowly migrating proteins, similar to the case with positively charged proteins. As for these proteins, the pH differences cause fronting which is more pronounced the higher the absolute mobility $|u_p|$ of the protein.

Conclusion: In most electrophoretic analyses of proteins, the tailing caused by conductivity differences is counteracted by fronting caused by pH differences, which decreases the peak asymmetry and, thus, the risk to obtain hyper-sharp peaks and loss in resolution (see Section 2.5.1).

2.8. Zone broadening caused by slow association–dissociation of a complex between a protein and a buffer constituent

A slow on/off kinetics gives rise to a distorted peak for reasons analogous to those causing tailing upon adsorption, the asymmetry increasing upon an increase in field strength. Observe, however, that the complex may become either less or more charged than the free protein. Accordingly, fronting, as well as tailing, may occur and both should increase with an increase in field strength. Protein/protein interactions can give a similar zone broadening. Examples are found in Ref. [16] (pp. 341–359) and Refs. [18,19].

2.9. Zone broadening caused by the curvature of the capillary

In a coiled capillary, the field strength is lower at the "outer lane" compared to that at the "inner lane", which manifests itself as a tilted zone [20]. For n complete loops, the zone broadening is $n2\pi d$ [20], which corresponds to the variance $\sigma_{curv}^2 = (1/4)(n\pi d)^2$ [21] or $(L_t d^2/16r_i^2)L_d$ [22] (d is the diameter of the capillary and r_i the sum of the internal radii of the capillary coils). The latter equation has been used in our calculations. In the HP^{3D} CE apparatus, the zones pass a $90°$ $+ 360° + 90°$ curvature of the capillary, contributing to the non-negligible variance 2.16×10^{-4} cm^2 for a capillary with the inner diameter $d = 50$ μm (see Table 1). For lysozyme with a diffusion coefficient of 1.1×10^{-6} cm^2/s, this variance corresponds to a diffusion (migration) time of 64 s (Eq. (2)). Consequently, the zone broadening caused by the curvature of the capillary may be significant in several commercial instruments. In microchip electrophoresis, where the zones sometimes pass several curvatures of the separation channel and the analysis times can be very short (seconds) and the diffusional zone broadening thus is negligible, the variance related to the curvature may be even more disturbing. This type of zone distortion is independent of the field strength. For a thorough discussion of the contribution of capillary coiling to zone dispersion, see the papers by Kašička et al. [22] and Gaš and Kenndler [23].

2.10. Novel equations

2.10.1. Zone broadening caused by sedimentation (convection) in capillary free zone electrophoresis

2.10.1.1. Quantitative treatment. Convective zone broadening, i.e., zone broadening caused by differences in density between the solute zone and that of the surrounding buffer, is seldom discussed in the HPCE literature. The likely reason is that a quantitative treatment has not been possible, since no equation has been published (to the best of our knowledge). Therefore, we present in this paper mathematical expressions, which were derived several years ago for an HPCE symposium but were never submitted for publication [5]. The equations are valid for the sedimentation of a zone in the vertical
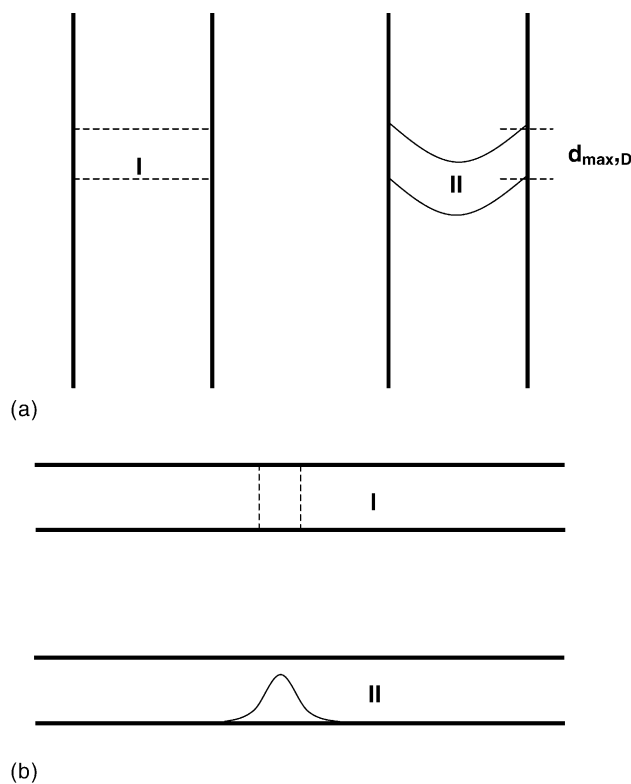
Fig. 2. Sedimentation of a zone in the vertical (a) and horizontal (b) section of the capillary. (I) The original shape of the zone. (II) The shape following sedimentation.

section of the capillary and take into account the decrease in zone broadening caused by radial diffusion. It can be shown that the shape of this zone is that of a parabola (Fig. 2a) with v_{maxD} (the maximum sedimentation velocity), d_{maxD} (the maximum migration distance) and σ_{sed}^2 (the variance) determined by the Eqs. (11)–(13), respectively.

$$v_{maxD} = \frac{R}{\sqrt{8Dt}}v_{max} = \frac{R^3 g}{8\eta\sqrt{2Dt}}(\rho_s - \rho_b) \tag{11}$$

$$d_{maxD} = \frac{R^3 g \sqrt{t}}{4\eta\sqrt{2D}}(\rho_s - \rho_b) \tag{12}$$

$$\sigma_{sedD}^2 = \frac{R^2 t}{96D}\left[\frac{gR^2}{4\eta}(\rho_s - \rho_b)\right]^2 \tag{13}$$

where g is the gravitational acceleration ($\sim$980 cm s^{-2}), ρ_s and ρ_b the densities of the sample and buffer solutions (g cm^{-3}), respectively, R the radius of the capillary (in our experiments, 0.0025 cm), D the diffusion constant of the protein (cm^{-2} s^{-1}), t the sedimentation time (s) and η the viscosity (0.01 poise for water at 25 °C).

The term convective broadening as used herein is an old notation (see for instance Ref. [24]). The same expression is, unfortunately, often used for the Taylor type of dispersions [7].

These equations are valid when $t \gg R^2/8D$, i.e., for a protein with $D = 1 \times 10^{-6}$ cm^2/s, the migration time must

be much longer than 0.8 s when $R = 0.0025$ cm. Accordingly, the equations are applicable to most separations with the exception of fast microchip analyses. The density difference in Eqs. (11)–(13) can be estimated from the relation [25]:

$$\rho_s - \rho_b = c(1 - \bar{v}_p \rho_b) \tag{14}$$

where c is the concentration of the solute ($\rho_s - \rho_b \approx 0.003$ g/cm^2 for a 1% protein solution), $\bar{v}_p$ = the partial specific volume of the solute (for proteins often 0.73 cm^3/g). It should be noted that the gravitational broadening has a parabolic velocity distribution with the apex pointing downwards (Fig. 2a). Therefore, a sedimenting zone is characterized by a tailing peak. Its shape is not primarily affected by the field strength and, therefore, neither is its variance, but indirectly since t in Eqs. (11)–(13) is inversely proportional to the field strength.

2.10.1.2. Sedimentation of the enriched protein zone. Plots of d_{maxD} (Eq. (12)) and σ_{sed}^2 (Eq. (13)) against time (t) for different protein concentrations are displayed in Fig. 3. We will first treat the case that the protein sample is applied electrophoretically under zone sharpening, i.e., the sample has an electrical conductivity much lower than that of the running buffer (see Section 2.10.2). The proteins will be efficiently trapped and enriched at the boundary between the lower and higher buffer concentrations (Fig. 4a, zone 1). This boundary is virtually stationary, which means that the enriched protein zone will become highly concentrated very close to the inlet of the capillary (see Section 3.7). Accordingly, there is a risk that part of the protein zone sediments out of the capillary. Even if the sedimentation distance is short during the time required for the application of the sample and for the subsequent washing of the inlet of the capillary, the percentage loss

(a)

(b)
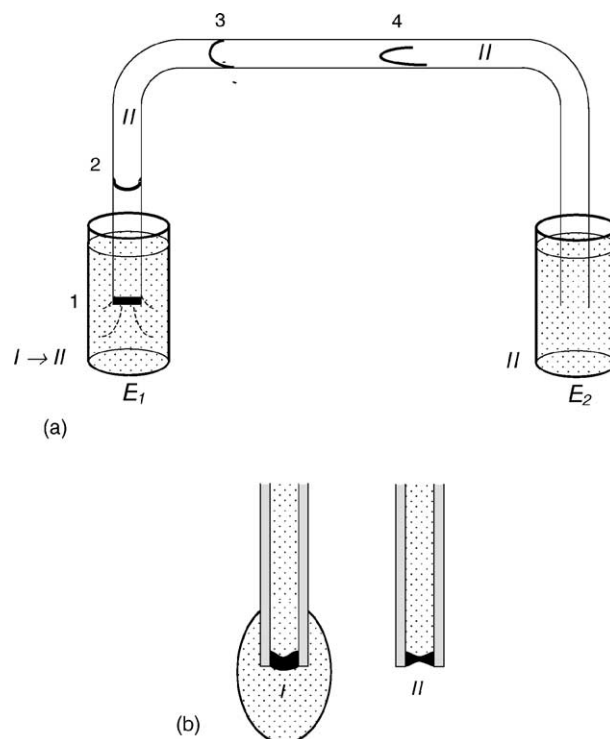
Fig. 4. (a) Enrichment and separation steps. In the enrichment step the electrode vial (E_1) is filled with the proteins to be analysed dissolved in diluted running buffer (phase I) and in the separation step with non-diluted running buffer (phase II). (1) Enriched sample zone (located close to the inlet); (2) zone distorted by sedimentation in the vertical section of the capillary (see Fig. 2a, II); (3) zone distorted by sedimentation becomes tilted when passing the first curvature of the capillary; (4) zone subjected to the above two distortions and sedimentation in the horizontal section of the capillary (Fig. 2b, II). (b) Loss of the sample during the enrichment (I) and washing (II) step.

(a) (b) (c) (d)
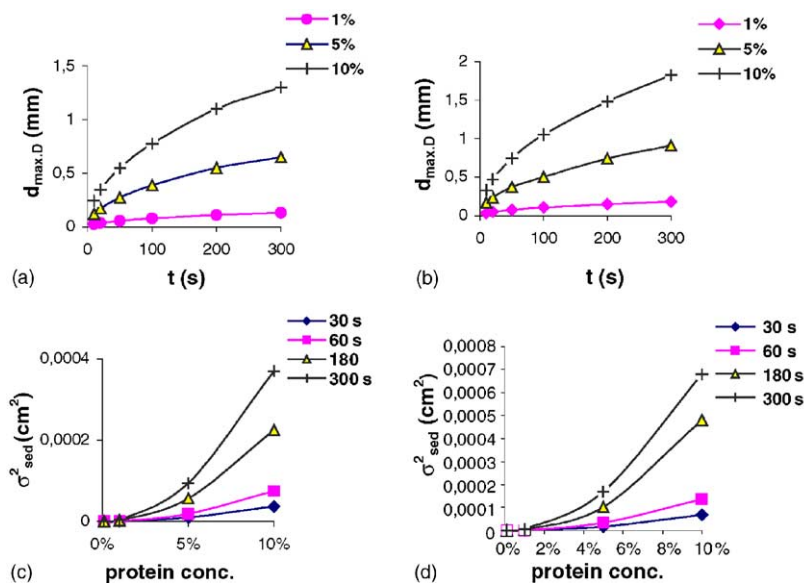
Fig. 3. (a and b) Plot of sedimentation distance (d_{maxD}) in a 50 μm capillary against the sedimentation time for a protein zone (a: lysozyme, b: albumin) at different protein concentrations (Eq. (12)) (see Sections 2.10.1.1 and 2.10.1.2 for the values of the experimental parameters). (c and d) Plot of the variance (σ_{sed}^2) against the protein concentration (c: lysozyme, d: albumin) (Eq. (13)).
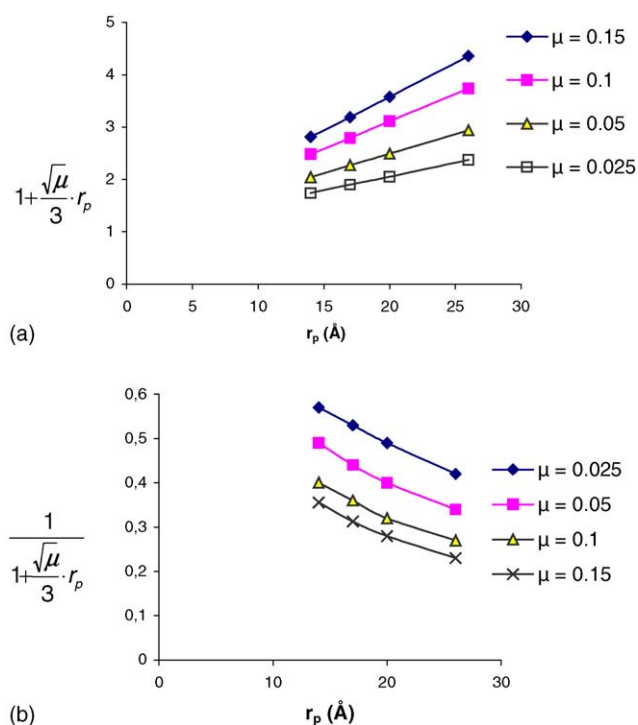
Fig. 5. (a) Plot of $\left[1 + (\sqrt{\mu}/3)r_p\right]^{II}$) against the radius ($r_p$) of the protein (see Eq. (20b)). This factor, multiplied by the ratio of the conductivities of non-diluted and diluted buffer (κ^{II}/κ^{I}), gives the enrichment factor (Eq. (20b)). (b) Plot of $1/(1 + \sqrt{\mu}/3)r_p$ against r_p. This factor multiplied by μ_0 (the mobility at infinite dilution) gives the mobility at the ionic strength μ (Eq. (19)). For molecular masses and radii, see Table 1 in Part II [1].

may be considerable, as estimated below (see also Fig. 4b). Assume that the sample consists of four proteins dissolved in the running buffer, diluted 100-, 500-, and 1000-fold and that the original concentration of each of the proteins is 0.1 mg/ml (see Fig. 10b, d, e in Part II [1]). The approximate Eqs. (18a) and (21) show that the concentration of each of the enriched proteins will be about 10, 50, and 100 mg/ml (totally 40, 200, and 400 mg/ml). Fig. 5 can be used to obtain more correct values. We also assume that the proteins do not separate during the enrichment and that the total time is 30 s for the contact between the diluted and non-diluted buffers at the inlet of the capillary in connection with the enrichment of the proteins, the washing of the capillary and all other procedures until the running voltage is applied. Insertion of appropriate parameter values into Eq. (12) for 100-fold dilution of the buffer [$\rho_s - \rho_b = 0.012$ g/cm^3 (4×0.003 g/cm^3), $t = 30$ s, $\eta = 0.01$ poise, $g = 980$ cm/s, $D = 1.1 \times 10^{-6}$ cm^2/s] gives $d_{maxD} = 0.17$ mm. For 500- and 1000-fold dilutions of the buffer $d_{maxD} = 0.80$ and 1.7 mm, respectively, although approximate. These values show that the risk that part of the enriched protein zone sediments out of the capillary cannot be neglected. No doubt, the subsequent washing of the capillary contributes to increasing the loss of protein (Fig. 4b, II).

The following alternative may be another explanation why the peak areas do not increase upon 500- and 1000-fold dilutions of the buffer. At extremely low BGE concentrations, the

buffering capacity is very low. The uptake of carbon dioxide from the air produces bicarbonate ions, which may increase the pH. The proteins in the sample, being ampholytes, can cause a change in pH, since the pH of a protein dissolved in pure water approaches the pI of the protein (see Section 2.7.2). In our experiments, the pH of the very diluted buffer may, therefore, be higher in the presence of the proteins, which causes a decrease in u_p^I in Eq. (17) and consequently in the enrichment factor. It has been suggested that a zone depleted of analyte ions forms in the vicinity of the tip of the capillary and that this decreases the enrichment factor. Open questions are: (1) whether this zone forms or to what extent in the presence of diffusion and (2) if formed will it be destroyed, for instance by convective flow in the sample solution generated by the density difference between the depleted zone and the surrounding buffer?

In view of the above considerations, it is not surprising that the peak areas did not increase when the dilution of the buffer increased from 100- to 1000-fold (Fig. 10Ba–Be in Part II [1]), nor that the repeatability was very poor. The concentrations of the proteins when they have separated into discrete zones are lower and, thus, d_{maxD} (see next section).

2.10.1.3. The loss of protein by diffusion and by thermal expansion of the buffer in the capillary. The linear thermal expansion of the buffer in the capillary is determined by the well-known expression $\Delta L = L\alpha\,\Delta t$, where α = the linear thermal expansion coefficient (= 0.6×10^{-4} for water). In Figs. 7b and 12b in Part II [1], the temperature rise were 7°C and 10°C, respectively (see Section 3.10 in that paper) i.e., $\Delta L = 48.4 \times 0.6 \times 10^{-4} \times 10(7) = 0.029(0.020)$ mm. A plug of 0.0145 mm and (0.01 mm) is thus pressed out of the capillary from its both ends, which may cause a partial loss of the enriched sample zone, since it is located at the virtually stationary concentration boundary at the tip of the capillary. This loss of protein is sometimes negligible, but not that caused by diffusion (see Section 3.7).

2.10.1.4. How to suppress the loss of protein upon enrichment?. These losses can be minimized if the stationary boundary is located at a somewhat longer distance from the inlet of the capillary by applying a narrow zone of the dilute buffer behind the sample dissolved in the dilute buffer. This modification can easily be introduced by pressure injection of a plug of the dilute buffer behind the sample.

2.10.1.5. Sedimentation of a zone during the run.

(a) The sedimentation of a lysozyme (albumin) zone in the *vertical* section of the capillary at 25°C contributes to the broadening with the variance 3.7×10^{-6} (6.9×10^{-6}) cm^2 if the migration time for lysozyme (albumin) in this section is 5 min and the protein has a concentration of 1% (see Fig. 5b in Part II [1]). The sedimentation variance is, accordingly, much smaller than the variances for diffusion and the curvature of the capillary, but similar to the variance of the thermal distortion (Table 1). The sedimentation distance d_{maxD}, following electrophore-

sis for 5 min in the vertical section of the capillary is 0.13(0.18) mm (see Fig. 3a and b). The sedimentation will thus not affect the accuracy in the determination of the mobility values, but will cause loss of protein and irreproducible peak areas at the sample application, as discussed in Section 2.10.1.2 and illustrated in Fig. 4b.

(b) A solute zone in the *horizontal* section of the capillary sediments at the same time as it spreads longitudinally along the bottom part of the inner wall of the capillary (Figs. 2b and 4a, zone 4) as visual inspection of a colored protein zone in capillaries with the diameters 1–3 mm indicated (rotation of the capillary eliminates this zone broadening [3,4,13]). The sedimentation decreases strongly with the diameter of the capillary, which, therefore, should not exceed 50 μm. Observe that it does not cause asymmetrical peaks, but increases, of course, with the sample concentration. The equation for the variance of this type of zone distortion has not been derived.

2.10.2. The enrichment factor

The conductivity of the sample is assumed to be lower than that of the running buffer. At the start of the run the entire capillary is filled with this buffer (phase II). One of the electrode vials (E_2) contains the same buffer (Fig. 4a). The other vial (E_1), filled with the same buffer diluted many-fold with water, contains the proteins to be analyzed (phase I). When voltage is applied, the proteins at the inlet of the capillary rush towards the virtually stationary boundary between the diluted and non-diluted buffers and become highly concentrated (zone 1 in Fig. 4a). The enrichment factor, ef, can be defined as the ratio between the protein concentrations in phases II and I following the enrichment:

$$ef = \frac{Q/\pi R^2 v_p^{II} t}{Q/\pi (\overline{R + \Delta R})^2 v_p^{I} t} \tag{15}$$

where Q is the amount of the protein transported from phase I to phase II; R the radius of the capillary; v_p^{I} the average electrophoretic velocity of the protein molecules when they migrate in phase I toward phase II; v_p^{II} the average electrophoretic velocity of the protein p in phase II; $\overline{R + \Delta R}$ the average effective radius of an imagined, truncated conical cylinder confining the protein molecules in phase I that migrate into phase II, t the time for the enrichment of the protein. Recalling that: $v = uE$ and $E = I/\kappa q$ (where I is the current and q the cross-sectional area of the capillary) Eq. (15) can be written:

$$ef \approx \left(\frac{\kappa}{u_p}\right)^{II} \left(\frac{u_p}{\kappa}\right)^{I} \tag{16}$$

We have here made the approximation that the field strength lines (see Fig. 4a) are parallel in the volume adjacent to the inlet of the capillary from which the sample ions migrate into the capillary, i.e., we have put $\Delta R = 0$. For a more rigorous treatment, one should employ the equation for the potential (in phase I) as a function of the distance from

the inlet of the capillary, as derived by Nolkrantz et al. [26]. Observe that Eq. (16) is exact when the protein, dissolved in the diluted buffer, is applied by pressure.

In fact, the *ef* value calculated from Eq. (16) is larger than the true one. In a set of experiments (such as that presented in Fig. 10 in Part II [1]) where the composition of phase II is unchanged, the ratio $(\kappa/u_p)^{II}$ is constant ($=C_{II}$). Accordingly, in this case, the expression can be simplified to:

$$ef \approx C_{II} \left(\frac{u_p}{\kappa}\right)^{I} \tag{17}$$

2.10.2.1. Case a: The mobility of the protein is about the same in phases I and II. This assumption is justified when the buffer in phase I is only slightly diluted. Eq. (16) then takes the simple form:

$$ef \approx \frac{\kappa^{II}}{\kappa^{I}} \tag{18a}$$

This equation has been derived for a protein, but the same relationship is, of course, valid for any charged solute, including buffer ions. Interestingly, using the Kohlrausch regulating function, which is based on the assumption that the mobilities of both protein and buffer ions are independent of the ionic strength, Longsworth has arrived at the same expression for moving boundary electrophoresis (Eqs. (11) and (12) in Chapter 3, by L.G. Longsworth [16]). Observe that in moving boundary experiments ΔR in Eq. (15) is zero.

A more exact formula than that derived by Longsworth is obtained if we apply Eq. (33) to a free zone electrophoresis experiment, putting $v^{\alpha\beta} = 0$ (the boundary is stationary):

$$ef = \frac{c_j^{\alpha}}{c_j^{\beta}} = \frac{v_j^{\beta}}{v_j^{\alpha}}$$

(for notations see Section 3.6).

For the above enrichment experiments, $j = p$, phase α = phase II, phase β = phase I, i.e.

$$ef = \frac{v_j^{I}}{v_j^{II}} = \frac{u_p^{I}(I/q\kappa^{I})}{u_p^{II}(I/q\kappa^{II})}.$$

Since I, the current, has the same value in all phases,

$$ef = \frac{u_p^{I}}{u_p^{II}} \frac{\kappa^{II}}{\kappa^{I}} \tag{18b}$$

an equation which is identical to Eq. (16).

2.10.2.2. Case b: The mobility of the protein differs in phases I and II. It is worth noting that the enrichment factor (Eq. (16)) increases upon dilution of phase I, not only because its conductivity, κ^{I}, decreases, but also because the mobility of the protein, u_p^{I}, increases (Fig. 12 in Ref. [2]). We will therefore derive an expression which gives a quantitative description in easily measurable parameters. To this end we combine Eq. (16) or Eq. (18b) with the

relationship (Eq. (18:13) in Ref. [14]):

$$u = \frac{u_0}{1 + Ar_p} \tag{19}$$

where u_0 is the mobility at infinite dilution, $(1/A)$ the thickness of the double layer ($\approx 3/\sqrt{\mu}$ Å [13], where μ is the ionic strength), and r_p the radius of the solute. The enrichment factor then takes the simple form

$$ef = \frac{\kappa^{II}}{\kappa^{I}} \frac{[1 + (\sqrt{\mu}/3)r_p]^{II}}{[1 + (\sqrt{\mu}/3)r_p]^{I}} \tag{20a}$$

In zone sharpening experiments, the ionic strength in the diluted buffer (phase I) is very low. Therefore, this expression can be simplified:

$$ef = \frac{\kappa^{II}}{\kappa^{I}} \left[1 + \frac{\sqrt{\mu}}{3}r_p\right]^{II} \tag{20b}$$

For spherical proteins, the ionic radius can be calculated from $r_p = (3\bar{v}M/4\pi N)^{1/3}$, where $\bar{v}$ is the partial specific volume of the protein (for most proteins $\bar{v} = 0.73$, except for glyco- and lipoproteins), M its molecular mass and N the Avagadro number. Using this equation and albumin as a reference protein ($r_p = 25$ Å, $M = 68\,000$), the radii of other proteins can roughly be estimated from the relation $r_p = 25(M/68\,000)^{1/3}$. This expression, although valid only for spherical proteins, was employed to calculate the ionic radii of the proteins used in experiments presented in Part II [1] (see Table 1 in Part II [1]). The dissymmetry factor f/f_0 was, accordingly, neglected. These ionic radii were also used to calculate the parenthesis in Eq. (20b) and plot it against the ionic radius (Fig. 5a). This graph, combined with κ^{II}/κ^{I} (the ratio between the conductivities of the non-diluted and diluted buffers), permits a rapid estimation of the enrichment factor for different ionic radii and ionic strengths (Eq. (20b)).

At the highest ionic strength in this example (0.15 M), the ef increases 1.8 times for proteins with $r_p = 14$ Å ($M \approx 12\,000$) and $r_p = 26$ Å ($M \approx 79\,000$). With decreasing ionic strength of the BGE, the effect is smaller.

The fact that also the mobility of a protein is a function of these parameters (Eq. (19)) means that the relative migration times of the proteins in a sample analyzed at a certain ionic strength differ from the relative migration times of the same proteins analyzed at another ionic strength (we assume here that at least some of the proteins have different ionic radii), which may increase the resolution between two adjacent protein zones. For a rapid estimation of the change in mobility of proteins with different ionic radii when the ionic strength is altered, see Fig. 5b, which gives the value of the factor $1/(1 + Ar_p) = 1/(1 + (\sqrt{\mu}/3)r_p)$ (Eq. (19)). Another reason to test various ionic strengths is that buffer constituents may form complexes with a protein and, thus, change its mobility and at best improve the resolution of proteins. Consequently, there are at least two reasons to analyze a protein mixture by capillary electrophoresis in buffers at different ionic strengths.

Whatever the reason, any change in the mobility of a protein will change the recorded peak area. Therefore, this area should be normalized by dividing it by the migration time to have it proportional to the amount of protein in the zone [27].

In many electrophoresis experiments, we are only interested in a rough estimation of the enrichment factor and can, therefore, put the parenthesis in Eq. (20b) equal to an average value of 2.5, or even 1, as we have done in some discussions herein, i.e., we have employed Eq. (18a) (and also the approximation that κ^{II}/κ^{I} is equal to the dilution factor).

At low ionic strengths in phase II, much lower than those used in the experiments in Part I and II [1] $((\sqrt{\mu}/3)r_p \rightarrow 0)$ Eq. (20b) becomes formally identical to Eq. (18a):

$$ef \approx \frac{\kappa^{II}}{\kappa^{I}} \tag{21}$$

i.e., the enrichment factor is then inversely proportional to the conductivity of the diluted buffer, or roughly inversely proportional to the dilution of the buffer. Observe the approximate nature of this expression, particularly as regards the assumptions that $\Delta R = 0$ in Eq. (18a) and that the ionic strengths are low in *both* phase I and phase II. In doubtful cases, Eqs. (20a) and (20b) are to be preferred; Fig. 5a gives a rapid estimation of the factor $1 + (\sqrt{\mu}/3)r_p$, part of the enrichment factor.

The original boundary between the buffer in the capillary (phase II) and the diluted buffer in the electrode vial (phase I) is a so-called concentration boundary, which in ideal electrophoresis, where one assumes that the ion mobilities are independent of the ionic strength, is stationary. In most experiments, this boundary moves slightly, as does the stationary zone in Fig. 1 (see Section 3.7). It should be stressed that all equations, including Eq. (19), describing the relation between mobility and ionic strength are approximate.

2.10.3. The migration time

2.10.3.1. Case 1: The sample is applied by electrophoresis. The experimental conditions are assumed to be identical to those described in Section 2.10.2 (see Fig. 4). Following the enrichment step, the concentrated zone is asymmetrical with the maximum concentration displaced toward the boundary created by the non-diluted and diluted buffer. We assume that the boundary has migrated a very short distance (ΔX_0) into the capillary upon electrophoretic application of the sample. Upon exchange of the diluted buffer in the electrode vessel (phase I) for the non-diluted buffer (phase II) and application of the running voltage, the sample zone starts to move faster. The following set of five equations permits calculation of the migration time t for the solute to reach the detection window:

$$t = \frac{L_d - (\Delta X_0/2)}{u_p^{II} E^{II}} \qquad \left(\frac{\Delta X_0}{2} \text{ is not well-defined}\right) \tag{22}$$

$$E^{II} = \frac{I}{\kappa^{II} q} \tag{23}$$

$$I = \frac{V}{r^{\mathrm{I}} + r^{\mathrm{II}}} \tag{24}$$

$$r^{\mathrm{I}} = \frac{\Delta X_0}{\kappa^{\mathrm{I}} q} \tag{25}$$

$$r^{\mathrm{II}} = \frac{L_{\mathrm{t}} - \Delta X_0}{\kappa^{\mathrm{II}} q} \tag{26}$$

i.e.:

$$t = \frac{(L_{\mathrm{d}} - (\Delta X_0/2))(\Delta X_0(\kappa^{\mathrm{II}}/\kappa^{\mathrm{I}}) + L_{\mathrm{t}} - \Delta X_0)}{u_{\mathrm{p}}^{\mathrm{II}} V} \tag{27}$$

where L_{d} is the length of the capillary to the detection window, L_{t} the total length of the capillary, ΔX_0 the width of the starting zone, E^{II} the field strength in phase II, κ the conductivity, q the cross-sectional area of the capillary, r the ohmic resistance, u_{p} the mobility of the protein and V the voltage over the capillary. For, $\kappa^{\mathrm{I}} = \kappa^{\mathrm{II}}$ Eq. (27) is reduced to

$$t = \frac{L_{\mathrm{d}} - (\Delta X_0/2)}{u_{\mathrm{p}}^{\mathrm{II}}(V/L_{\mathrm{t}})} = \frac{L_{\mathrm{d}} - (\Delta X_0/2)}{u_{\mathrm{p}}^{\mathrm{II}} E^{\mathrm{II}}} \tag{28}$$

which is the well-known expression for calculation of the migration time when the sample is dissolved in a non-diluted running buffer.

Since $\Delta X_0/2 \ll L_{\mathrm{d}}$ and $\Delta X_0 \ll L_{\mathrm{t}}$ (see Table 1 and Section 3.7 in this paper and Tables 6 and 7 in Part II [1]), Eq. (27) can be simplified:

$$t = \frac{L_{\mathrm{d}}(\Delta X_0(\kappa^{\mathrm{II}}/\kappa^{\mathrm{I}}) + L_{\mathrm{t}})}{u_{\mathrm{p}}^{\mathrm{II}} V} \tag{29}$$

The term $\Delta X_0 \kappa^{\mathrm{II}}/\kappa^{\mathrm{I}}$ is not negligible in zone sharpening experiments when the sample is dissolved in a strongly diluted running buffer. In a series of such experiments, it is likely that the values of ΔX_0 vary considerably, particularly because they are very small, in some cases less than 0.1 mm (see Table 1 in this paper and Tables 6 and 7 in Part II [1], as well as Section 3.7).

2.10.3.2. Case 2: The sample is applied by pressure.

$$t = \frac{\Delta X_0}{u_{\mathrm{p}}^{\mathrm{I}} E^{\mathrm{I}}} + \frac{L_{\mathrm{d}} - (\Delta X_0/2)}{u_{\mathrm{p}}^{\mathrm{II}} E^{\mathrm{II}}}. \tag{30}$$

Using the same approach as in case 1, one obtains

$$t = \frac{\Delta X_0[\Delta X_0 + (\kappa^{\mathrm{I}}/\kappa^{\mathrm{II}})(L_{\mathrm{t}} - \Delta X_0)]}{u_{\mathrm{p}}^{\mathrm{I}} V}$$

$$+ \frac{(L_{\mathrm{d}} - (\Delta X_0/2))[\Delta X_0(\kappa^{\mathrm{II}}/\kappa^{\mathrm{I}}) + (L_{\mathrm{t}} - \Delta X_0)]}{u_{\mathrm{p}}^{\mathrm{II}} V} \tag{31}$$

Eq. (27) is, however, most often applicable to both cases 1 and 2, since, in practice, the first term in Eq. (31) is negligible in the majority of CE experiments, because in zone sharpening experiments $\kappa^{\mathrm{I}} \ll \kappa^{\mathrm{II}}$ and often $\Delta X_0 < 1$ mm (see Table 1 and Section 3.7).

The difficulty to define ΔX_0 in a simple way and exactly has the consequence that calculations of terms where ΔX_0 is a parameter are very approximate.

Immediately after the enriched zone has passed the concentration boundary, it starts to broaden and become more asymmetrical, the larger the conductivity jump, $\Delta\kappa$, i.e., the higher is the analyte concentration and the larger is the difference in mobility between the analyte and the buffer co-ion (see Eqs. (7) and (19)). Notice that pH differences, as well as interactions between the protein and the buffer may decrease the asymmetry (see Sections 2.7 and 3.2). Thermal zone broadening may also contribute to the asymmetry as can adsorption of the analyte onto the capillary wall.

In the discussion above, we have assumed that the voltage over the capillary is kept constant. Therefore, the current changes during the run because of variations in the conductivity in the area around the concentration boundary at the inlet of the capillary. The migration velocity varies accordingly, which may affect the reproducibility. However, if the power supply delivers constant current this problem will not occur. An additional advantage of constant current is that the migration velocities are independent of variations in temperature (pp. 178–182 in Ref. [4]) and the presence of small bubbles and precipitates in the capillary, and is, therefore, recommended for most electrophoresis experiments.

3. Discussion

3.1. Quantified zone broadenings

The width of the starting zone (ΔX_0) and, thereby, the variance $[(\Delta X_0)^2/12]$ can easily be determined experimentally in the conventional way from velocity and migration time when the sample is equilibrated with the buffer. If this is not the case, for instance when the sample is subjected to zone sharpening, the variance can be determined experimentally from a plot of plate height against $1/E$ (see Section 2.1 and p. 681 in Ref. [2]).

The variance of diffusional (Eq. (2)), thermal (Eq. (5)) and convective (Eq. (13)) zone broadening and that of the curvature of the capillary [21–23] can easily be calculated. If one (or more) of the above variances is (are) much larger than the other variances, one should try to minimize that (those) variance(s). In the experiments presented in Table 1, the variances corresponding to longitudinal diffusion are much larger than the other variances, with the possible exception of the variance of the curvature of the capillary (in the present design of the cartridge the curvature is fixed, unfortunately). The most obvious and efficient ways to diminish the diffusional zone broadening is to increase the field strength, provided that the thermal effects on zone broadening and bubble formation do not become disturbing and/or to shorten the capillary if some resolution can be sacrificed. Alternatively, one can use low-conductivity buffers [28] or hybrid micro devices [29].

The width of a zone and the zone broadening (2σ at 60% of peak height and $\sqrt{12}\sigma$ for the width of the starting zone)

are listed in Table 1, particularly because they give a visual picture of the performance of a run, whereas the variance does not. This intuitive feeling that the zone width is a measure of the quality of a separation is reflected in the mathematical inverse proportionality between resolution and zone width.

The experimentally determined width of the α-chymotrypsinogen zone in the experiment presented in Table 1 was only 1 mm and the inevitable zone broadening caused by diffusion 0.77 mm. All other types of zone broadening were smaller. These data clearly indicate that capillary electrophoresis is a true high-performance method, provided that the practical experiments are designed in accordance with the current theory, discussed in this paper. Observe that the sum of the separate zone widths is not equal to the total zone width (only independent variances are additive).

Table 1 shows that the difference between the experimentally determined total variance and the sum of the calculated variances was about 28% of the variance of diffusion in the most successful runs. Which zone distortions give rise to the additional (rest) variance? This question is dealt with in Section 3.3.

If the sum of the above calculated separate variances is larger than the total variance, the zones have been narrowed by some kind of zone sharpening. It should be emphasized that variances determined experimentally in the presence of electroosmosis may be much lower than those determined in the absence of electroosmosis (p. 680 in Ref. [2]). Examples on protein separations in a capillary with electroosmotic flow (EOF) will soon be published [30]. "Apparent" plate numbers determined in the presence of electroosmosis (N_{ep}) can be recalculated to "true" plate numbers obtained in the absence of electroosmosis (N_{ep+eo}) by means of a simple equation: $N_{ep} = (u_{ep}/(u_{ep} \pm u_{eo}))^2 N_{ep+eo}$ (Eq. (79) in Ref. [2]). Instead of using the terms true and apparent plate numbers, it may be more appropriate to state that plate numbers should be compared under similar experimental conditions, when possible in the absence of electroosmosis.

The thermal and convective zone distortions cause zone broadening. However, a zone distortion, for instance a tailing, does not always give rise to zone broadening. Examples are given in the next section. Observe that tailing is a necessary but not a sufficient condition for adsorption.

3.2. Different types of zone distortions which do not cause (significant) zone broadening and, therefore, need not be quantified

This category comprises distortions caused by reversible adsorption, association–dissociation processes, isomerization, etc. when the on/off kinetics is fast, and differences in conductivity and pH between sample zone and buffer (see Section 3.6). However, in experiments where these distortions give rise to a hyper-sharp boundary the broadening of one boundary of the zone is not compensated by a sharpening of the other boundary (see Sections 2.5.1 and 2.6). Such zone distortions cause strongly asymmetrical peaks and may
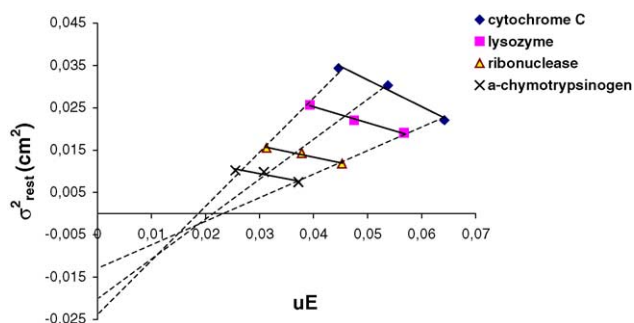
Fig. 6. Plots of the rest variance σ^2_{rest} against uE. For definition of rest variance, see Table 1. BGE: ammonium acetate, pH 4.0 (ionic strength: 0.12 M). Full lines: u constant, E varies (see Section 3.3.2). Broken lines: E constant, u varies (see Section 3.3.1).

contribute considerably to the total variance. Observe that conductivity and pH differences often counteract each other (see Sections 2.7.1 and 2.7.2).

3.3. The rest variance discussed in terms of Eq. (6)

The rest variance in the plot in Fig. 6 is the total, experimentally determined variance minus the sum of the calculated variances listed in Table 1, i.e., the rest variance corresponds to all other interactions the analyte can be involved in, for instance with buffer constituents and sedimentation of the zone in the horizontal section of the capillary, and to peaks where one boundary is hyper-sharp (see Section 2.5.1). Observe that a hyper-sharp boundary may be blurred by thermal, convective and other distortions and, therefore not show up in the electropherogram as a line prependicular to the baseline.

3.3.1. The rest variance as a function of uE, when E is constant and u varies, i.e., corresponding to an electrophoresis experiment with different proteins (the broken lines in Fig. 6)

The three straight broken lines in Fig. 6 were obtained for each of the three electrophoresis experiments with the first four proteins in Table 1 in Part II [1] (BGE: ammonium acetate, pH 4). This relationship is not expected if the proteins interact with the capillary wall, since it would mean that the constant C in Eq. (6) has the same value for different proteins which is very unlikely. This conclusion is supported by the finding that the *relative* migration velocities of these four proteins changed in accordance with Eq. (19) for different ionic strengths (see Section 3.2.1 in Part II [1]), which indicates that proteins do not adsorb onto polyacrylamide-coated capillaries, not even the basic ones (see Eq. (6)).

However, ions as small as ammonium ions very likely interact electrostatically similarly with, for instance, carboxylic groups in different proteins, and acetate ions with, for instance amine groups, i.e., the constant C in Eq. (6) should have the same value for most proteins (we assume here that Eq. (6) is valid not only for adsorption but also for other interactions). Accordingly, the straight broken lines in Fig. 6 probably represent interactions between

buffer constituents and proteins. An indirect support for this conclusion is the observation in Part II [1] and many other articles that different buffers often give different electropherograms.

Somewhat hydrophobic buffer ions and such which interact selectively with the proteins to be analyzed can be expected to alter the appearance of the electropherograms and, thus, affect the resolution more than simple ions. The constant C in Eq. (6) may under such conditions have different values for different proteins and the broken line in Fig. 6 will not be straight. The interactions must not be so strong (slow) that the peaks become heavily distorted (for instance hyper-sharp).

3.3.2. The rest variance as a function of uE, when u is constant and E varies, i.e., corresponding to electrophoresis experiments of a certain protein at different field strengths (the full lines in Fig. 6)

The data are taken from the experiments displayed in Fig. 6. For each of the four proteins, the rest variance (= the variance for all interactions each protein takes part in interactions with other proteins, buffer constituents, capillary wall) decreases when the field strength increases.

This is not expected for protein/capillary wall interactions (see Eq. (6))—another support for the indications, presented in the previous section, that this type of interaction is negligible. However, one can very well imagine that the contact time for the interaction between small buffer ions and a protein (suggested in Section 3.3.1) is shorter in the presence of an electrical field than in the absence of it which is in agreement with the above observation that the variance decreases with an increase in field strength. In fact, we started some years ago chromatographic experiments with superimposed alternating or direct voltage to decrease the C-term in the van Deemter equation. An interesting question is whether the kinetics may be faster at increasing voltage by a mechanism analogous to that described by Tallarek et al. [31].

The observation that electrophoresis in different buffers of the same pH may give different separation profiles and plate numbers is not only an argument for the existence of interactions between protein and buffer constituents, but also an indication that the choice of buffer is a critical step in the pursuit of high resolution. From moving boundary experiment it is well-known that small molecules can interact with proteins [16]. Recently, capillary electrophoresis was used to study the interaction between lysozyme and the anions citrate and phosphate [18,19]. Phosphate ion was used as buffering constituent in experiments shown in Part II [1].

To conclude: Eq. (6) is valid for protein/buffer interaction only when E is constant and u varies, accordingly, for each electrophoresis experiment with proteins (the broken lines in Fig. 6), at least for proteins of similar molecular weights, but not when u is constant and E varies, i.e., not for electrophoresis of a certain protein at different field strengths (the full lines in Fig. 6).
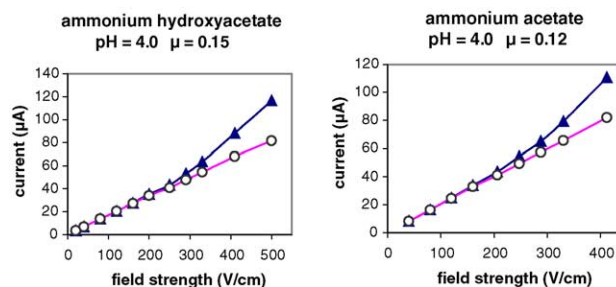
Fig. 7. Plots of current against field strength.

3.4. What is the optimum field strength?

The ratio between the variance for thermal zone deformation in the presence of radial diffusion (Eq. (5)) and in its absence (Eq. (53a) in Ref. [2]) is ($R^2/8Dt$). For α-chymotrypsinogen ($D = 0.9 \times 10^{-6}$ cm^2/s at 25 °C) analyzed in a 50 μm capillary for 15 min, the ratio is 10^{-3}. Can we expect radial diffusion to decrease the variance that much? The plot of current against voltage in Fig. 7 shows that the deviation from the straight line (caused by Joule heating) becomes evident already at 247 and 268 V/cm for ammonium acetate and ammonium hydroxyacetate, respectively, and is very pronounced at 360 V/cm, the field strength used in our experiments. In spite of this, Eq. (5) gives a very small, negligible variance, 3.04×10^{-6} cm^2 (Table 1). It should be added that the highest plate numbers (1 660 000 and 1 600 000 per meter) were attained in these experiments, although the difference between the experimental and the critical field strengths was large (360/247 and 360/268 for ammonium acetetate and ammonium hydroxyacetate, respectively, see Table 4 in Part II [1] and also the discussion herein in Section 2.3)

Could we have used a still higher voltage in our experiments without increasing significantly the thermal zone broadening, or does the radial diffusion not decrease this zone broadening as much as the Taylor approach predicts? This is an important question, since a higher field strength means a shorter migration time, i.e., a smaller diffusional broadening – and diffusion gives the largest contribution to the total zone broadening (Table 1 herein and Section 4 [1]). Thorough theoretical and experimental studies are required to answer the above question. Several researchers have found that thermal zone distortions often are negligible [8,32,33].

3.5. Zone broadening in free zone electrophoresis compared to that in chromatography, including electrochromatography

The presence of a stationary medium is a prerequisite for all chromatographic separations, whereas in free zone electrophoresis the experiments are conducted in buffer alone. Eddy diffusion and the attendant zone broadening (corresponding to the A-term in the van Deemter equation) thus arises only in chromatography, but not in carrier-free electrophoresis. The stationary phase makes the longitudinal diffusion (described by the B-term in the van Deemter

equation) somewhat restricted in chromatography and therefore causes a smaller zone broadening compared to that in free zone electrophoresis. In gel electrophoresis, the diffusion is still more restricted.

Separations in chromatography, but not those in electrophoresis, are based on the interaction between sample constituents and a stationary phase (the *C*-term in the above equation). The on/off kinetics for the interaction is usually relatively slow, which may cause considerable peak broadening. An interaction between a buffer constituent and the solute gives rise to a considerable peak broadening in both electrophoresis and chromatography when the kinetics is slow. An example from the field of moving boundary electrophoresis is the complex formation between ovalbumin and acetate ions under acidic conditions [16]. For electrophoretic broadening caused by protein/protein or protein/nucleic acid interactions, isomerization or polymerization, see pp. 341–359 in Ref. [16].

The chromatographic zones will become more narrow if a packed, particulate bed is replaced by a less heterogenous stationary phase, such as a continuous bed, also called a monolith [34]. Electrochromatography in a homogenous gel should give zones as narrow as those typical of gel electrophoresis, provided that the on/off interactions of the solute with the ligands attached to the polymer chains in the gel are rapid enough [35].

It is well-known that many solutes adsorb strongly onto the wall of bare fused silica capillary to cause peak tailing. It should be stressed that this adsorption originates from both electrostatic and hydrophobic interactions (and others), which means that adsorption is not necessarily diminished by changing the ionic strength of the buffer, because an increase of the ionic strength to suppress electrostatic interactions increases the hydrophobic interactions, and vice versa [36]. The most general method to eliminate both adsorption and electroosmosis and with the great advantage of imposing few restrictions of the choice of buffer and ionic strength, might be that based on a large increase of the viscosity in the double layer by applying a hydrophilic neutral polymer coating [3,4], which gives a negligible adsorption also of basic proteins, probably the most strongly adsorbing class of biopolymers (Part II [1]). Therefore, one can expect the polyacrylamide coating to be appropriate for all classes of analytes, provided that the capillary is washed at low pH between the runs (Part II [1]).

Thermal zone deformation appears both in electrophoresis, caused by Joule heat, and chromatography, caused by frictional heat, but is at moderate flow rates negligible in the latter method. The onset of the deviation from a straight line in a plot of current against voltage indicates the field strength at which the Joule heat becomes measurable. However, this field strength is lower than the field strength that gives optimum resolution (Fig. 7 in Ref. [2]). It should be recalled that with special low-conductivity buffers one can use field strengths as high as 2000 V/cm or higher without any thermal distortion [28]. Such high field strengths

require good electrical insulation to avoid spark formation [28,29].

Conclusion: From the above comparison between electrophoretic and chromatographic zone broadening, it might be evident that free electrophoresis and particularly gel electrophoresis theoretically gives narrower zones, i.e., higher plate numbers than does chromatography, assuming that the experimental conditions for these methods have been chosen so as to give a minimum in total zone broadening (optimum conditions). Therefore, it is not surprising that some of the plate numbers we obtained in the CE study published in Part II [1] are, to the best of our knowledge, considerably higher (up to 1 700 000 per meter, see Table 1) than those achieved in chromatographic experiments. The width of this protein zone in the capillary at the detection window was 1 mm—a remarkably narrow zone as obtained in a capillary with 40 cm effective length. The very high plate numbers reported in electrochromatography for charged compounds in packed silica columns might have their origin in zone-focusing gradients [37] (plate numbers are defined for isocratic conditions and, therefore, difficult to interpret in gradient systems). Observe that electrochromatography of charged analytes which do not interact with the stationary phase gives a separation pattern similar to the pattern obtained in capillary free zone electrophoresis (CE) in an uncoated capillary, i.e., in the presence of electroosmosis provided that the analytes do not interact with the capillary wall. The plate numbers obtained in CEC may, therefore, be much higher than those obtained in CE in the absence of electroosmosis, although the widths of the zones in the capillaries may be similar (p. 680 in Ref. [2]). A later study has shown that the peak compression for cationic analytes in CEC using cation exchangers occurs predominantly when the analyte, injected in a medium deviating from the electrolyte by a higher concentration of organic solvent, has a similar elution time as the EOF (see Figs. 2 and 5 in Ref. [38]). The analyte elutes in a zone where the migration speed is faster than in the surrounding buffer, and will consequently be enriched at the boundary where the speed slows down.

3.6. *Different types of zone distortions which give rise to asymmetrical peaks in electrophoresis, chromatography, electrochromatography, and (ultra) centrifugation, but little or no loss in resolution of two adjacent peaks, provided that one boundary of a zone is not hyper-sharp*

Assume that an analyte molecule moves by diffusion from phase α to phase β across boundary I and that the electrophoretic velocity is higher in the α-phase compared to that in the β-phase (Fig. 8b). This molecule will eventually move back into the α-phase, provided that $v_j^\alpha > v_j^\beta$. Analogously, a molecule at boundary II, which by diffusion enters the β-phase, will successively move away from boundary II, i.e., the peak will become asymmetrical with tailing. However, the broadening of boundary II will be about the same as the sharpening of boundary I, i.e., the width of the asymmetrical peak in Fig. 8b will be similar to that of the symmetrical peak
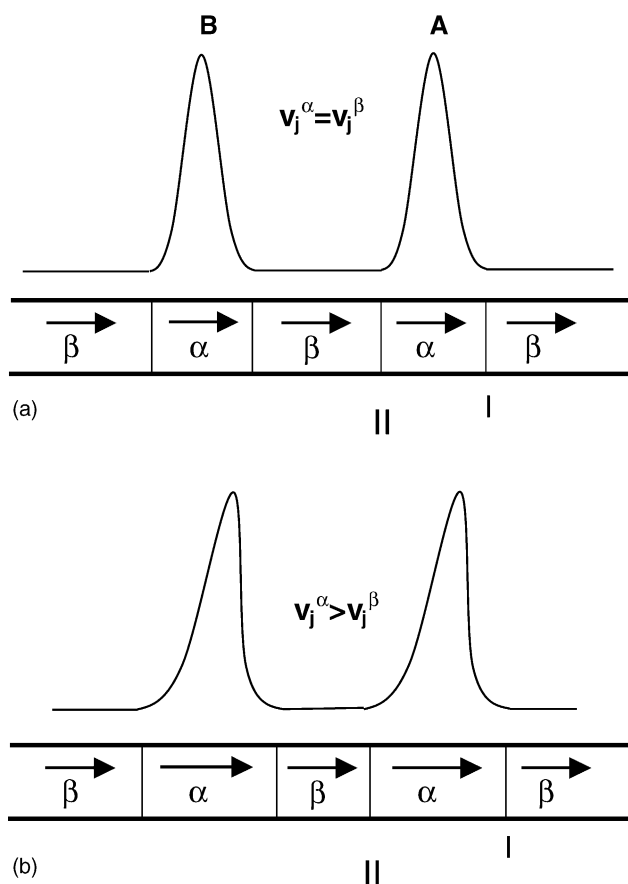
Fig. 8. Peak distortion caused by moderate differences in conductivity or pH between the analyte zone and the surrounding buffer do not, or only slightly, contribute to peak broadening. (a) Peak A is symmetrical since we assume that there are no differences in the migration velocity of sample ion j in phases α and β ($v_j^\alpha = v_j^\beta$). Peak B is an adjacent peak, i.e., its migration velocity is similar to that of peak A and therefore it is also virtually symmetrical. (b) Distorted peaks caused by differences in migration velocities of sample ion j in phases α and β ($v_j^\alpha > v_j^\beta$). Assume that an analyte ion j in the α-phase at the boundary II diffuses into adjacent β-phase. Since the velocity of ion j is lower in β-phase compared to that in the α-phase, this analyte ion will move slower, i.e., boundary II will broaden. Analogously, if an analyte ion j at boundary I diffuses into the adjacent β-phase, the boundary I will sharpen. Accordingly, peak A becomes asymmetrical and the sharpening of boundary I will become virtually equally as large as the broadening of boundary II, i.e., the asymmetrical peaks in the experiment (b) have the same widths as the symmetrical peaks in experiment (a). Peak B is an adjacent peak, i.e., its migration velocity is similar to that of peak A and therefore it has virtually the same asymmetry as peak A. Accordingly, the resolution of the asymmetrical peaks in (b) is similar to the resolution of the symmetrical peaks in (a). The above statements refer to electrophoresis, chromatography, and electrochromatography.

obtained when the migration velocities are the same in phases α and β (Fig. 8a); and equally important, the resolution of two adjacent peaks will be the same independently of whether the peaks are symmetrical or asymmetrical. However, when a large peak separates from an adjacent, very small one (e.g., in protein impurity studies) the small peak may be symmetrical (Eq. (7), low c_p) affecting the resolution.

The situation becomes different when boundary I cannot become sharper (it is hyper-sharp), whereas boundary II continues to become more and more blurred, i.e., the peak successively becomes wider. Characteristic of a hyper-sharp boundary in an advancing or rear profile is the appearance of a straight rise or descent perpendicular to the baseline. Such a sharp boundary is seldom observed in an electropherogram, since "softer" boundaries corresponding to other distortions of the boundary are superimposed.

The above reasoning can be applied to any separation method based on differences in transport velocities of the analytes, i.e., for electrophoresis, chromatography, electrochromatography, and (ultra) centrifugation. The difference in velocity of the analyte j in phases α and β may be caused by differences in conductivity and pH, complex formation, isomerization, adsorption, partition, etc.

We can now make the following generalization: small differences in electrophoretic, chromatographic, electrochromatographic and gravitational velocities of a solute within a zone and outside cause peak asymmetry due to a combination of fronting and tailing effects. However, the width of a zone will be about the same as for a symmetrical peak, as will the resolution between two adjacent peaks.

Considering the above mentioned causes of the differences in migration velocity of the analyte j in phases α and β, it is obvious that, in practice, it may be very difficult to get a perfectly symmetrical peak in any separation method, particularly with macromolecules. For instance, in free capillary electrophoresis it might be impossible to find a coating which eliminates completely interactions with all types of proteins, but this is not necessary in order to get high resolution (high plate numbers), provided that the on/off kinetics is fast enough, as emphasized in Section 3.2. Observe that the above discussion of different types of zone broadening is based on the parameter velocity. Using this parameter, one can make a further generalization and derive an expression which is valid for all the four methods mentioned in the heading (Eq. (98) in Ref. [2]):

$$c_j^\alpha v_j^\alpha - c_j^\beta v_j^\beta = (c_j^\alpha - c_j^\beta)v^{\alpha\beta} \tag{33}$$

where c_j^α and c_j^β are the concentrations of the ion j in the α- and β-phases, respectively; v_j^α and v_j^β are the velocities of the ion j in the α- and β-phases, respectively, and $v^{\alpha\beta}$ is the speed of the moving boundary separating the phases α and β. Since this equation (Eq. (33)) is valid for both electrophoresis, chromatography, electrochromatography, and (ultra) centrifugation, one can immediately state that all types of electrophoretic zone distortions discussed herein (for instance those based on complex formation, differences in conductivity and pH between the sample zone and the BGE) have counterparts in chromatography, electrochromatography and centrifugation. In other words: these four analysis methods have analogous (but not similar) properties: for instance, any phenomenon appearing in electrophoresis appears also in chromatography in an analogous way (and vice versa).

3.7. Estimation of the migration velocity of the "stationary" concentration boundary

In a zone sharpening experiment, Eq. (33) can be written as

$$c_j^\alpha v_j^\alpha - \frac{c_j^\alpha}{n} v_j^\beta = \left(c_j^\alpha - \frac{c_j^\alpha}{n} \right) v^{\alpha\beta} \tag{34}$$

where n is the dilution factor. Accordingly,

$$v_j^\alpha - \frac{v_j^\beta}{n} = \left(1 - \frac{1}{n} \right) v^{\alpha\beta} \tag{35}$$

Since

$$v = uE = \frac{u_0}{1 + (\sqrt{\mu}/3)r_j} \frac{I}{q\kappa},$$

Eq. (35) can be transformed to

$$v^{\alpha\beta} = \frac{v_j^\alpha - (v_j^\beta/n)}{1 - (1/n)}$$

$$= \frac{Iu_0}{q(1 - (1/n))} \left[\frac{1}{(1 + (\sqrt{\mu^\alpha}/3)r_j)\kappa^\alpha} \right.$$

$$\left. - \frac{1}{n(1 + (\sqrt{\mu^\beta}/3)r_j)\kappa^\beta} \right] \tag{36}$$

κ_j^β need not be known, since $n\kappa_j^\beta \approx \kappa_j^\alpha$. Eq. (36) can therefore be simplified:

$$v^{\alpha\beta} = \frac{Iu_0}{q(1 - (1/n)\kappa^\alpha)}$$

$$\times \left[\frac{1}{1 + (\sqrt{\mu^\alpha}/3)r_j} - \frac{1}{1 + (\sqrt{\mu^\beta}/3)r_j} \right] \tag{37}$$

Using the data from the experiment in Fig. 5a in Part II [1], along with $\kappa^\alpha = 6.18 \times 10^{-3}\,\Omega^{-1}\,cm^{-1}$, $I = 85 \times 10^{-6}\,A$, $r_{NH_4^+} = 1.4$ Å, $u_{NH_4^+} = 33 \times 10^{-5}\,cm^2\,s^{-1}\,V^{-1}$ $= |v^{\alpha\beta}| = 0.019\,cm/s$, corresponding to the mobility $5.3 \times 10^{-5}\,cm^2\,s^{-1}\,V^{-1} = 5.3$ T units [39], i.e., the migration distance of the concentration boundary following a 20 s injection is thus 0.38 cm. However, the diffusion of the protein (cytochrome C) during the injection and the additional time before the running voltage is applied (totally 30 s) gives a broadening $(2\sigma) = 0.2\,mm$ (Eq. (2)), i.e., the width of the stationary zone is determined also by diffusion, and not only by the migration distance of the concentration boundary. Interestingly, the mobility of the concentration boundary is 7.3 fold lower than the mobility of the ammonium ion. The above results indicate that one can use diffusion alone for sample application. In fact, we have employed this technique for many years, particularly for capillary chromatography. Observe that $v^{\alpha\beta}$ is proportional to Iu_0 and that the ammonium ion has an extremely high mobility. Using ions with lower mobility and lower, more commonly employed buffer concentrations, the product Iu_0 can be reduced 100-fold and consequently also $v^{\alpha\beta}$, i.e., the concentration boundary will be located very close to the tip of the capillary with attendant consequences (see for instance Section 2.10.1.2).

3.8. Limitations in the application of the Kohlrausch regulating function (the ω-function), exemplified by restrictions in the use of Eq. (7), and a brief description of an alternative regulating function (the H-function)

To facilitate somewhat the mathematical treatment Eq. (7) was derived for simple buffers, such as ammonium acetate [13], a BGE used in some of the experiments presented in Part II [1], although a similar equation, of course, can be derived for any type of buffer. In fact, the theory of the moving boundary electrophoresis suffers from the same basic inaccuracy as Eq. (7), namely that it is strictly valid only for strong electrolytes, since the derivation is based on the Kohlrausch regulating function (the ω-function) which has this restriction. However, this function has been used with great success to explain the electrophoretic behavior of proteins, particularly in combination with the use of effective mobilities (see Section 1.4.5 in Ref. [13]). The reason for the success is that the pH and ionic strength are approximately constant throughout the separation medium (see Refs. [16,24] as well as [13], where also the derivation of Eq. (7) is given and, therefore, illustrates under which conditions this equation is valid).

The *H*-function $\left(\sum c_j v_j \right)$, which is derived from Eq. (33), has the same value in all phases ($H^\alpha = H^\beta = \cdots$), as has the ω-function ($\omega^\alpha = \omega^\beta = \cdots$), but has the advantage that the mobility of an ion need not be the same in all phases [40].

4. Conclusions

Table 1 is a compilation of data for α-chymotrypsinogen, from which one can draw the following important conclusions:

(1) Longitudinal diffusion causes the largest zone broadening. The most obvious and efficient way to reduce the total zone broadening further is, therefore, to decrease the run time, i.e., simply shorten the capillary (if a lower resolution can be accepted) or increase the field strength without increasing the zone broadening caused by Joule heating (see also Section 3.4.). This can be accomplished if the capillary is in contact with a massive supporting plate, preferably one made of a ceramic with a high electrical but low thermal resistance. This hybrid microdevice permits run times which are 15-fold shorter than those in conventional CE apparatus without loss in resolution [29]. Another alternative is to replace the conventional buffers by low-conductivity buffers which allow field strengths above 2000 V/cm without generating disturbing Joule heat [28].

(2) All other kinds of zone broadenings besides those considered in Table 1 have together a variance (rest variance) which is about 28% of that caused by diffusion alone. These various types of zone broadening refer to different kinds of interactions (for instance protein/protein, protein/buffer ion), sedimentation in the horizontal section of the capillary (Fig. 2b) and zone distortions caused by so large conductivity and pH differences between a protein zone and surrounding buffer that one boundary is hyper-sharp. The latter distortions often counteract each other and, therefore, hyper-sharp peaks seldom appear in electrophoretic separations of proteins. Protein/capillary wall interactions seem to be negligible.

To obtain plate numbers per meter as high as 1.7×10^6 (Table 1), the experiments described in Part II [1] show that much attention should be paid to the choice of: (1) the method used to coat the inner wall of the capillary, (2) the procedure for washing the capillary between the runs, and (3) the background electrolyte and its concentration and pH. Very likely, we did not manage to find the optimum conditions. An obvious question is then how much higher plate numbers than those we have observed can be attained and what is the gain in resolution. The theoretical maximum plate number is that which is based on the sum of all inevitable variances, in our experiments those originating from diffusion and the curvature of the capillary, i.e., $N_{max} = L_d^2/(\sigma_{diff}^2 + \sigma_{curv}^2)$.

The resolution is proportional to $\sqrt{N}$ and the maximum increase in resolution is, accordingly,

$$\frac{\sqrt{N_{max}} - \sqrt{N_{exp}}}{N_{exp}} \times 100\%$$

$$= \frac{\left(L_d/\sqrt{\sigma_{diff}^2 + \sigma_{curv}^2}\right) - (L_d/\sigma_{exp})}{L_d/\sigma_{exp}} \times 100\%$$

$$= \left(\frac{2\sigma_{exp}}{2\sqrt{\sigma_{diff}^2 + \sigma_{curv}^2}} - 1\right) \times 100\%.$$

Insertion of relevant values (Table 1) gives

$$\left(\frac{0.98 \times 10^{-1}}{2\sqrt{1.43 \times 10^{-3} + 2.16 \times 10^{-4}}} - 1\right) \times 100\% = 20.8\%.$$

Even if this figure becomes somewhat higher (26.6%) if we use a CE apparatus where the curvature of the capillary is smaller, the question is whether it is worth all the efforts we have to devote to increasing the resolution further (see the two points above), since the gain in resolution will still become relatively limited.

An important conclusion is that plate numbers which exceed the plate numbers we have obtained by more than 20–30% indicate zone sharpening effects, provided that the run times are the same as in our experiments. The extremely high plate numbers observed in electrochromatography have been explained by such phenomena [37] or by the fact that electrophoresis of charged analytes in the presence of electroosmosis gives "apparent" plate numbers which are higher than the plate numbers determined in the absence of electroosmosis, although the zone widths may be larger [2].

5. Guidelines for the design of high-performance CE experiments

The discussions herein and the experiments in Part II [1] give us some clues about how to proceed to create successful experiments, including high plate numbers.

(1) Choose a CE-apparatus where the capillary is straight or only slightly curved.
(2) In the case of UV detection, choose separation media (buffer, polymer solution, gel) with low UV absorption for detection at 200–220 nm to increase the sensitivity (for instance, gels of low-melting agarose are, from this point of view, preferable to those of polyacrylamide [41]).
(3) Test buffers of different compositions, concentrations and pH and choose the buffer that gives the highest plate number and/or resolution in the subsequent optimization steps.
(4) Use low field strengths for the application of the sample.
(5) Do several experiments at different field strengths in this buffer to find out which field strength gives the highest resolution. This critical field strength is much higher for low-conductivity buffers [28] and hybrid microdevices [29].
(6) Calculate the variance for zone distortions when formulae are available (see Table 1). If one or more of these variances are considerably larger than the others, change the experimental values of relevant parameters in these formulae in order to decrease the variance(s). Calculate the width (2σ, at 60% of peak height and $\sqrt{12}\sigma$ for the starting zone) from these variances to get an idea about the width corresponding to the different variances.
(7) Plot the difference between the experimentally determined total variance and the sum of the calculated variances (the rest variance) against the field strength. The rest variance may correspond to variances caused by hyper-sharp boundaries and interaction-based variances, for instance between the protein and buffer constituents, other proteins, the capillary wall, etc., i.e., interactions which can be expected to increase with an increase in the field strength (see Eq. (6)). If this plot indicates interactions, use relatively low field strengths, try to decrease these interactions by conducting the experiments in other buffers and wash the capillary with 2 M HCl.
(8) On the other hand, if the rest variance decreases with an increase in field strength (see Fig. 6, full lines),

increase the field strength which has the additional advantage that the diffusional zone broadening (which in the experiments presented herein contributed to the total variance more than other zone distortions) decreases.

(9) Pay attention to the peak shapes when zone sharpening techniques are used, and avoid so high analyte enrichments that hyper-sharp peaks develop, resulting in excessive zone broadening.

(10) If you know of some interesting phenomenon in chromatography (for instance, one which increases the resolution) an analogous phenomenon exists also in electrophoresis and can be utilized in this separation method, as well.

Acknowledgements

References

[1] S. Mohabbati, S. Hjertén, D. Westerlund, J. Chromatogr. A 1053 (2004) 201.
[2] S. Hjertén, Electrophoresis 11 (1990) 665.
[3] S. Hjertén, Almqvist & Wiksells Boktryckeri, Uppsala, 1967.
[4] S. Hjertén, Chromatogr. Rev. 9 (1967) 122.
[5] S. Hjertén, manuscript in preparation.
[6] R. Virtanen, Zone electrophoresis in a narrow-bore tube employing potentiometric detection: a theoretical and experimental study, Acta Polytech. Scand., Helsinki, 1974.
[7] G. Taylor, Proc. R. Soc. 219 (1953) 186.
[8] S.V. Ermakov, P.G. Righetti, J. Chromatogr. A 667 (1994) 257.
[9] R.J. Wieme, in: E. Heftmann (Ed.), Chromatography, A Laboratory Handbook of Chromatographic and Electrophoretic Methods, Van Nostrand Reinhold, New York, 1975, p. 228.
[10] B. Gaš, M. Štědrý, A. Rizzi, E. Kenndler, Electrophoresis 16 (1995) 958.
[11] M. Štědrý, B. Gaš, E. Kenndler, Electrophoresis 16 (1995) 2027.
[12] H. Poppe, Adv. Chromatogr. 38 (1998) 260.
[13] S. Hjertén, in: G. Milazzo (Ed.), Topics in Bioelectrochemistry and Bioenergetics, 2, Wiley, 1978, p. 89.
[14] C.J.O.R. Morris, P. Morris, Separation Methods in Biochemistry, Pitman, London, 1976.
[15] O. Stålberg, D. Westerlund, U.B. Rodby, S. Schmidt, Chromatographia 41 (1995) 287.
[16] M. Bier, Electrophoresis, Academic Press, New York, 1959.
[17] X. Xu, W.T. Kok, H. Poppe, J. Chromatogr. A 742 (1996) 211.
[18] L. Kremser, E. Kenndler, G.I.T. Lab. J. 1 (2004) 23.
[19] M. Rabitter-Baudry, BIO Forum Eur. 3 (2004) 30.
[20] T. Srichaiyo, S. Hjertén, J. Chromatogr. 604 (1992) 85.
[21] S. Wicar, M. Vlenchik, A. Belenkii, A.S. Cohen, B.L. Karger, J. Microcolumn Sep. 4 (1992) 339.
[22] V. Kašička, Z. Prusík, B. Gaš, M. Štědrý, Electrophoresis 16 (1995) 2034.
[23] B. Gaš, E. Kenndler, Electrophoresis 23 (2002) 3817.
[24] H. Svensson, Ark. Kemi, Miner. Geol., 22A, no. 10 (1946) 1. Thesis.
[25] J.W. Williams, K.E. van Holde, R.L. Baldwin, Chem. Rev. 58 (1958) 715.
[26] K. Nolkrantz, C. Farre, R.I.D. Karlsson, A. Brederlau, C. Brennan, P.S. Eriksson, S.G. Weber, M. Sandberg, O. Orwar, Anal. Chem. 73 (2001) 4469.
[27] S. Hjertén, K. Elenbring, F. Kilár, J.-L. Liao, A. Chen, C. Siebert, M.D. Zhu, J. Chromatogr. 403 (1987) 47.
[28] S. Hjertén, L. Valtcheva, K. Elenbring, J.-L. Liao, Electrophoresis 16 (1995) 584.
[29] Á. Végvári, S. Hjertén, Electrophoresis 24 (2003) 3815.
[30] S. Mohabbati, S. Hjertén, D. Westerlund, manuscript in preparation.
[31] U. Tallarek, M. Paÿes, E. Rapp, Electrophoresis 24 (2003) 4241.
[32] J.H. Knox, K.A. McCormack, Chromatographia 38 (1994) 207.
[33] A.S. Rathore, K.J. Reynolds, L.A. Colón, Electrophoresis 23 (2002) 2918.
[34] S. Hjertén, Ind. Eng. Chem. Res. 38 (1999) 1205.
[35] S. Hjertén, Á. Végvári, T. Srichaiyo, H.X. Zhang, C. Eriksson, D. Eaker, J. Cap. Electrophoresis 5 (1998) 13.
[36] S. Hjertén, J. Chromatogr. 87 (1973) 325.
[37] N.W. Smith, M.B. Evans, Chromatographia 41 (1995) 197.
[38] A.M. Enlund, M.E. Andersson, G. Hagman, J. Chromatogr. A 979 (2002) 335.
[39] N. Catsimpoolas, S. Hjertén, J. Porath, Nature 259 (1976) 264.
[40] S. Hjertén, C. Eriksson, Y.M. Li, R. Zhang, Biomed. Chromatogr. 12 (1998) 120.
[41] S. Hjertén, T. Srichaiyo, A. Palm, Biomed. Chromatogr. 8 (1994) 73.
[42] Z. Zhao, A. Malik, M.L. Lee, Anal. Chem. 65 (1993) 2747.
[43] M. Gilges, H. Kleemiss, G. Schomburg, Anal. Chem. 66 (1994) 2038.
[44] H. Wan, M. Öhman, L.G. Blomberg, J. Chromatogr. A 924 (2001) 59.